ANALYSIS OF IRRADIATED CONCRETE

REPORT 2016:239

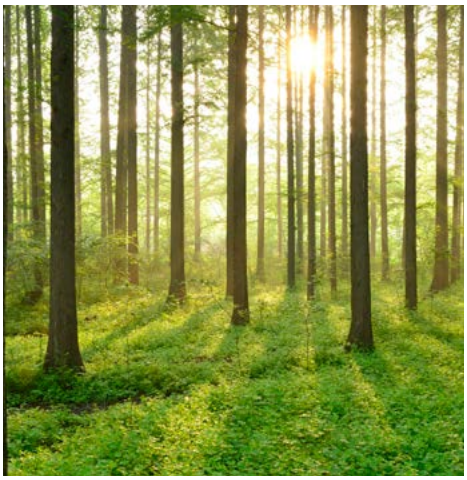

NUCLEAR CONCRETE RESEARCH PROGRAMME

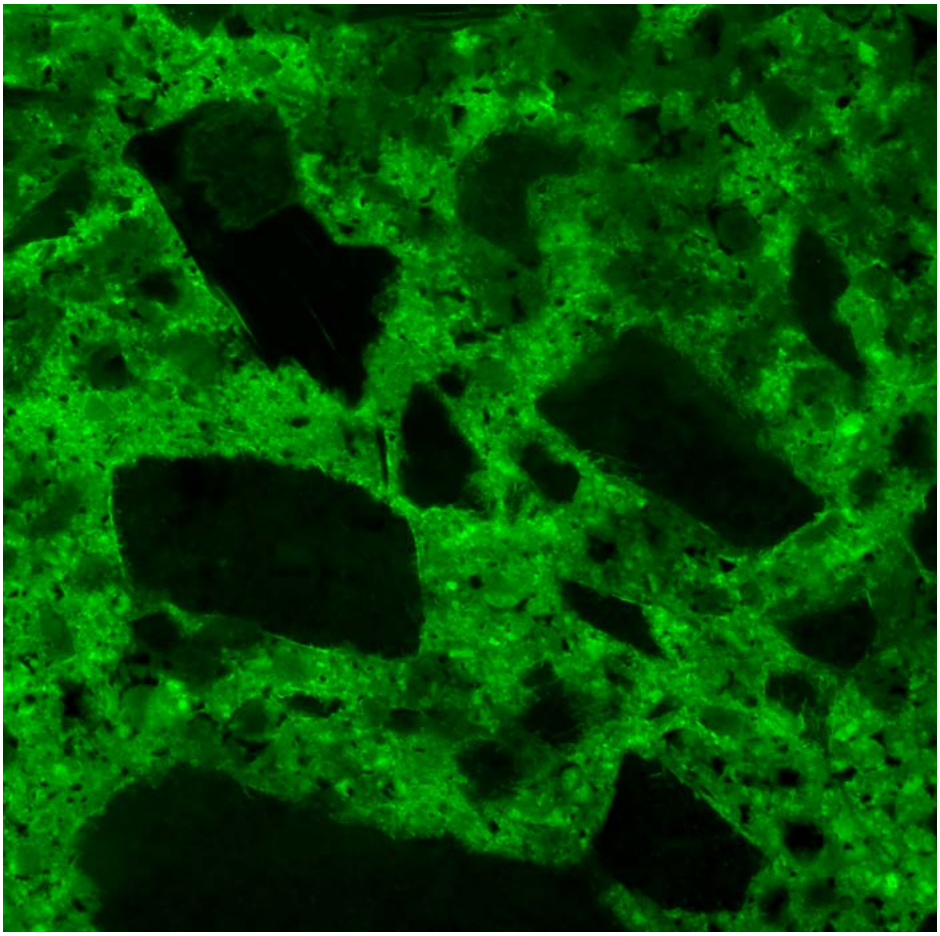

Energiforsk

Analysis of irradiated concrete

Microscopic and mechanical tests on concrete from a nuclear power plant containment structure

JAN ERIK LINDQVIST, CBI, MATHIAS FLANSBJER, SP AND ERIK HANSSON, INSPECTA

ISBN 978-91-7673-239-7 | © 2016 ENERGIFORSK

Energiforsk AB | Phone: +46 (0)8-677 25 30 | E-mail: kontakt@energiforsk.se | www.energiforsk.se

Foreword

Irradiation effects on concrete is a subject that has drawn more and more attention, as the possible life time extension of nuclear power plants beyond original design life is discussed.

Oskarshamn Nuclear Power plant (OKG) has initiated a project to analyse drilled concrete cores from the containment of Oskarshamn 2. Analysis using optical microscopy and scanning electron microscopy was performed. Given the international interest in this type of investigation, the Energiforsk Nuclear Concrete research program initiated a further development and translation of the original report that was submitted to OKG in Swedish.

The aim of the Energiforsk Nuclear Concrete research program is to initiate research and development that will contribute to a safe and cost effective long term operation of Swedish and Finnish nuclear power. The program is financed by Vattenfall, E.ON, Fortum, Skellefteå Kraft, Karlstads Energi, Strålsäkerhetsmyndigheten (SSM) and Teollisuuden Voima Oy (TVO).

Sammanfattning

De gjorda undersökningarna har inte påvisas något som tolkas som förändringar i betongen som är specifika för miljön där proverna tagits. De skillnader man kan påvisa i betongytan jämfört med betongens inre delar är sådana att bedömningen är att motsvarande förändringar kan ske i betong i normal inomhusmiljö. Det finns inga tecken på att strålning orsakat expansion i ballasten eller uttorkningskrympning av cementpastan. Det finns inget som tyder på att miljön inneburit förändringar som försämrar de mekaniska egenskaperna. Den skada som finns i ytan på prov 5 bedöms som orsakad av mekanisk påverkan och påverkan är ytlig och lokal.

Betongens mekaniska egenskaper utvärderades genom enaxiella tryckförsök på cylindrar bearbetade från utborrade kärnor.

Under tryckförsöket registrerades deformationsfältet på ytan av cylindrarna med ett optiskt mätsystem. Principen för detta system bygger på att två högupplösta kameror tar en serie bilder av provobjektet under provning. Bilderna analyseras sedan med s.k. korrelationsanalys (Digital Image Correlation - DIC). Den grundläggande idén bakom metoden är att mäta deformationen av ett objekt under belastning genom att analysera hur mönstret i diskreta fasetter på objektets yta deformeras.

Att det förekommer vissa variationer i töjning mellan de olika segmenten är naturligt eftersom styvheten lokalt beror på aggregatens storlek och placering. Den generella bilden är dock att töjningsfördelningen är relativt jämn utefter cylinderns längd vilket tyder på att de provade cylindrarna inte uppvisar någon degradering av mekaniska egenskaper. Det är heller ingen signifikant skillnad mellan cylindrar tagna mot insidan jämfört med cylindrar tagna mot utsidan

Den sammantagna slutsatsen är att de utförda provningarna inte pekar på någon degradering av materialets mekaniska egenskaper, samt att egenskaperna i stort är likvärdiga för kärnorna tagna mot insidan och mot utsidan av konstruktionen.

Summary

Drilled concrete cores from the central part of the containment structure of reactor 2 in Oskarshamn were tested in the present study. Optical microscopy and scanning electron microscopy were applied.

The microscopy analyses performed have not documented any changes in the properties of the concrete that can be interpreted as being due to the specific environment to which the samples have been exposed. The parameters that have been studied include crack patterns that could indicate volume changes in the aggregate or cement paste and indications of alkali silica reaction. The observed differences in the concrete surface compared to the inner part of the concrete are such that they could occur in concrete exposed to a normal indoor environment. There are no crack patterns to indicate that the radiation has caused a volume increase in the aggregate or drying shrinkage in the cement paste. There are no changes in the crack patterns, porosity or polarization properties that may indicate reduced mechanical strength. The damage seen in the surface of sample 5 is likely to have been caused by a local mechanical impact and this damage is superficial and local.

The mechanical properties of the concrete were evaluated by uniaxial compression tests on cylinders machined from drilled cores. Full-field strain measurement was performed on the surface of the cylinders during the compression test. Optical full-field deformation measurement was conducted using a measurement technique based on Digital Image Correlation (DIC) with a stereoscopic camera set-up, consisting of two CCD cameras. The basic idea behind DIC is to measure the deformation of the specimen during testing by tracking the deformation of a surface speckle pattern in a series of digital images acquired during loading.

That there is some variation in strain between the various segments is natural, since the local stiffness depends on aggregate size and location. The general picture is that the strain distribution is relatively uniform along the length of the cylinder, which indicates that the tested cylinders do not exhibit any degradation of mechanical properties. There is also no significant difference between the cylinders taken towards the inside of the structure, compared with those taken towards the outside.

The overall conclusion is that the tests carried out do not indicate any degradation of the mechanical properties, and that the properties in general are equivalent for the cores taken towards the inside and the outside of the structure.

List of content

1 Introduction

During the autumn of 2013 the PLEX modernization project at reactor 2 in Oskarshamn involved core drillings in the central part of the containment structure. The work was performed primarily to enable fastening of essential safety equipment. This created a great opportunity to investigate the status of the concrete in the reactor containment close to the reactor tank. Reactor 2 is of the BWR type and was commissioned in 1975.

For the PLEX project the most interesting aspect to investigate was the mechanical properties of the concrete. Extensive calculations were performed to structurally verify the plant, and this was a great opportunity to verify the calculation assumptions through testing. Degeneration of the concrete due to unique environmental circumstances is also of great interest for the long-term operation of the plant.

The performed tests show a very low level of degeneration and the mechanical properties show good agreement with the literature for predicting aging.

2 Sampling

The core drillings were performed at the HC wall that forms part of the biological shield surrounding the reactor tank. The HC wall consists of a 9 m high circular structure with a diameter of 14 m and a thickness of 700 mm. The wall was cast in 1972 with slow-hardening standard Portland cement and a concrete grade of BTG 1 LH _P_T K400. The structure is reinforced with KS40-s rebar on a typical c-c spacing of 300 mm. The surface is painted with epoxy paint. During normal operation the containment is filled with nitrogen.

In total, 18 core drillings were performed with a diameter of 80 mm and a length of 700 mm. However to execute the drilling the cores were broken in half, creating an inner and an outer part of each sample.

Directly after the samples were extracted they were put into plastic bags that were sealed to avoid direct contact with the air.

The colour coating on the concrete surface was ground off before the samples were transported to Borås. The samples used for the micro-analysis were marked 1 2.2 and 5 respectively. The samples are shown in figure M-1 and figure M-2.

Figure M-1. The drilled core marked 1 2.2.

Figure M-2. The drilled core marked 5.

3 Microscopy method

The samples were analysed in an optical polarization fluorescence microscope (PFM) using thin-section technique. Optical PFM microscopy applied in this study is a widely accepted method for the identification of alkali silica reaction (ASR) in concrete. The water-cement ratio was assessed by comparison with reference samples of known water-cement ratio according to the method NT BUILD 361. This method is based on assessment of the intensity of fluorescence light, which increases with increasing capillary porosity. Fluorescence microscopy can identify sub-micrometre cracks. This makes it possible to identify expansion of aggregate at an early stage. The combination of microscopy and mechanical testing is described in Flansbjer et al., 2011.

Micro-chemical analyses were performed in a low-vacuum scanning electron microscope equipped with an energy-dispersive detector for micro-chemical analysis, LVSEM/EDS.

4 Short introduction to the research field

This introduction is largely based on the report "A review of the Effects of Radiation on Microstructure and Properties of Concretes Used in Nuclear Power Plants" by Kaspar, Yunping, Naus and Graves (2013), and the report "Degradering av betong och armering med avseende på bestrålning och korrosion" by P Ljustell and J Wåle, SSM rapport 2014:31, http://www.stralsakerhetsmyndigheten.se/Global/Publikationer/Rapport/Sakerhet-vid-karnkraftverken/2014/SSM-Rapport-2014-31.pdf and references in these two publications.

Both neutron and gamma radiation can/may break covalent bonds. This process can transform quartz from crystalline to successively more amorphous material. One result of this is that the quartz-bearing aggregate becomes more ASR reactive. As a result non-reactive aggregate may become ASR reactive (Ichikawa and Koizumi 2002). A management programme for ASR damage has been proposed by Sauma and Hariri-Ardebili (2014).

The breakage of the covalent bonds leads to an increase in volume of the aggregate. The same process leads to a decrease in the volume of the cement paste. If these volume changes are sufficient to reduce the strength of the concrete they would produce cracks radiating out from the expanding aggregate. Such crack patterns are possible to identify at an early stage using fluorescence microscopy.

The radiation may cause carbonation through radiolysis, in which decomposition of the pore solution subsequently leads to carbonation. This type of carbonation is not restricted to developing from the surface inwards, but may also initiate within the concrete. The radiation-induced carbonation does not result in an increase in the mechanical strength of the concrete, as is the case for conventional carbonation of Portland cement paste.

Radiation may also increase the temperature in concrete. In a concrete reactor containment and shield structures the temperature does not exceed 65°C when the reactor is running normally. The exception is close to pipe penetrations where the temperature limit is 95°C. Temperatures below 65°C are too low to cause any damage to the concrete in an otherwise dry non-concrete-aggressive environment.

These radiation-induced processes may lead to a reduction in the mechanical strength of the concrete. This was investigated by Hilsdorf and others in the 1960s and 1970s and summarized by Hillsdorf et al. (1978). Later research has shown that the type of accelerated tests applied in these early investigations does not compare with the situation in practical applications. The temperature in the early experiments was unrealistically high. This has led to further research over the last 15 years on the effects of radiation on the strength of concrete. This includes experiments and modelling (e.g. Le Pape et al., 2015) as well as the development of evaluation systems (Maruyama et al., 2013). The present report concerns prediction of the service life of nuclear power plants. This issue has received considerable research attention recently. Emphasis in this summary of the research field is thus on the most recent publications.

5 Optical PFM microscopy

5.1 CORE 1 2.2

The concrete in the sample is based on Portland cement as binder. Based on the fluorescence intensity, which reflects the capillary porosity, the water-cement ratio was estimated at 0.5. The air content in the concrete is low and the air voids are well rounded.

The cement paste in the concrete surface has a slightly darker colour in the outermost 0.5 to 2.5 mm. There is a 0.3 mm thick surface layer with more dense cement paste (figure M-3). In this layer the relative proportion of unhydrated cement clinker minerals is higher (figure M-4). There are also small irregular pores in this layer. The diameter of the pores is in the range 10 to 50 microns. The outermost part of the sample is composed of an uncarbonized cement mortar with limestone filler. Most of this cement mortar was ground off during the preparation of the samples before they were allowed to be removed from OKG. The aggregate that has been exposed in the concrete surface has cracks that are assessed to be dynamic cracks caused by grinding during sample preparation. These cracks had propagated to a maximum depth of 0.5 mm. The micro-crack frequency in the cement paste is very low. Cracks in the adhesion zone around the aggregate particles are rare. Micro-cracks radiating out from aggregate particles that would indicate an increase in the volume of the aggregate particles were not observed. A typical example is given in figure M-5.

The aggregate is composed of granite and gneisses of granitic composition, as well as amphibole-bearing gneisses. There are also a few aggregate particles that are assessed to be potentially alkali silica reactive (ASR). The percentage of such particles is however far below the limit at which the aggregate would be assessed as potentially reactive. There are no signs of ASR reaction in the sample. No change in the polarization properties was observed in the cement paste or aggregate near the concrete surface.

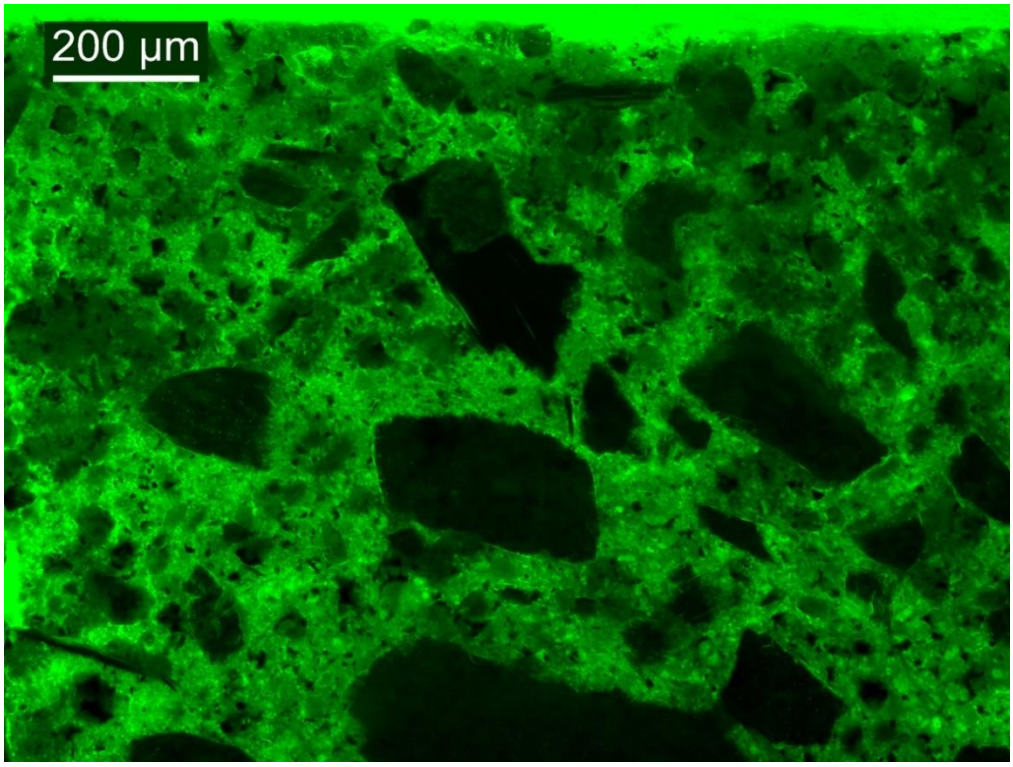

Figure M-3. Fluorescence image that shows the denser cement paste near the concrete surface in sample 1 2.2.

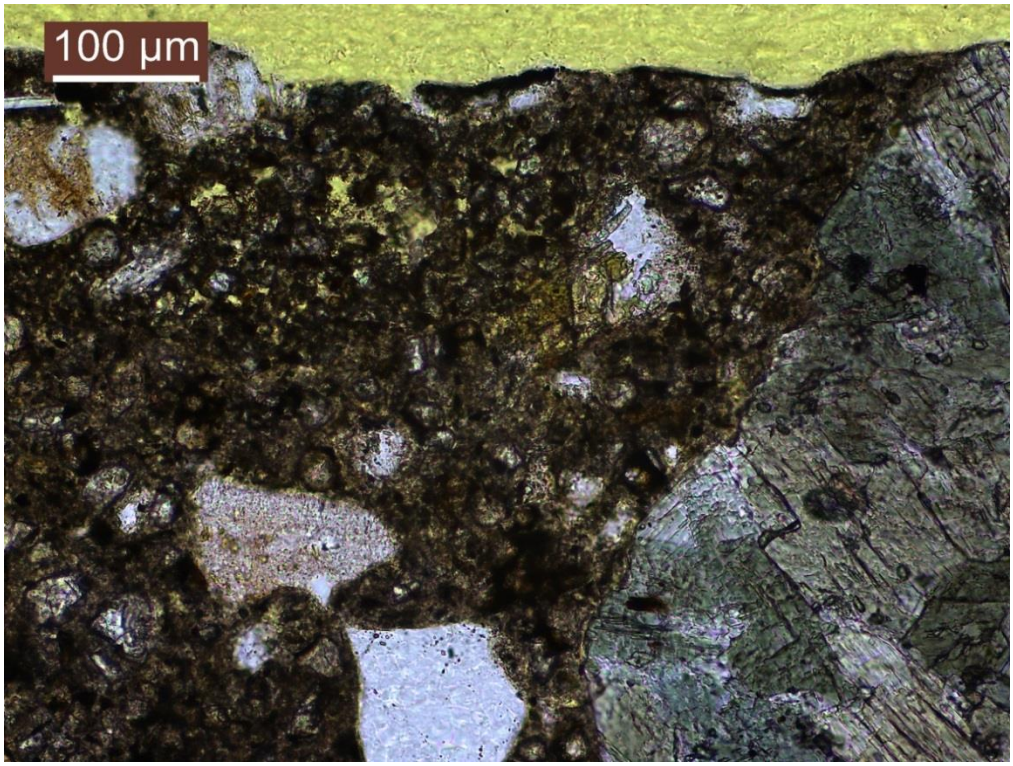

Figure M-4. Microscope image taken in plain light. The images show the surface layer with unreacted cement clinker and irregular voids close to the concrete surface in sample 1.

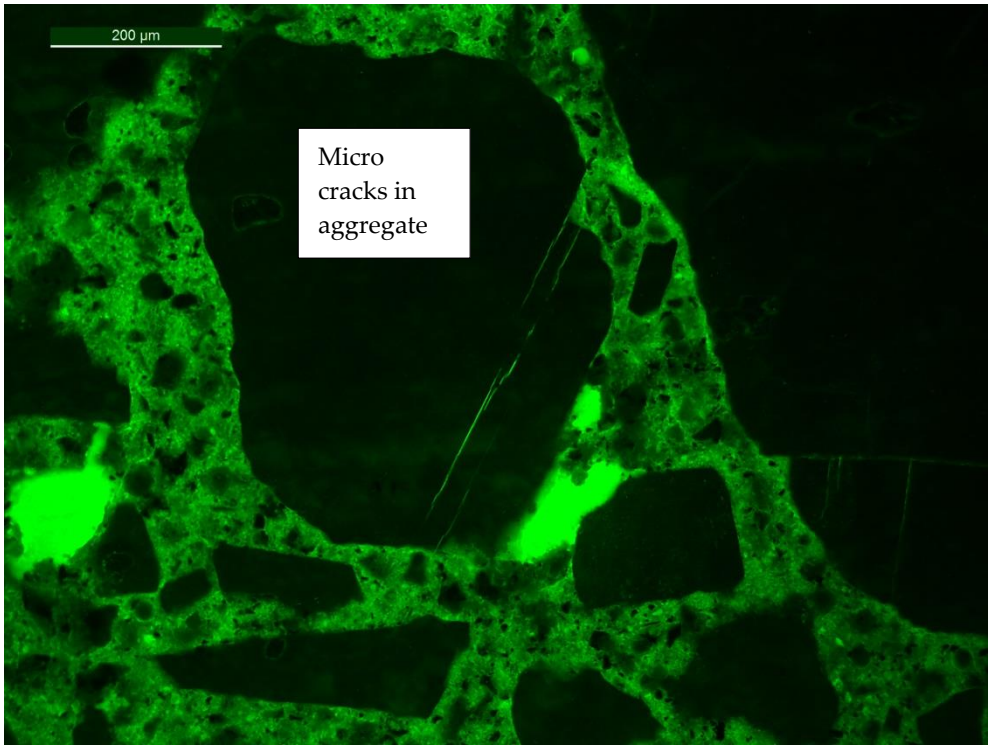

Figure M-5. Fluorescence image that shows internal micro-cracks that do not propagate into the cement paste.

5.2 CORE 5

The concrete in the sample is based on Portland cement as binder. Based on the intensity fluorescence, which reflects the capillary porosity, the water-cement ratio was estimated at 0.45. The air content is low and the voids are well rounded.

The aggregate is composed of granite and gneisses of granitic composition as well as amphibole-bearing gneisses. There are also a few aggregate particles that are assessed to be potentially alkali silica reactive (ASR). The percentage of such particles is however far below the limit at which the aggregate would be assessed as potentially reactive. There are no signs of ASR reaction in the sample. No change in the polarization properties was observed in the concrete surface.

The micro-crack frequency in the cement paste is very low. Cracks in the adhesion zone around the aggregate particles are rare. Micro-cracks radiating out from aggregate particles that would indicate an increase in the volume of the aggregate particles were not observed.

There is a paint layer on the concrete surface. It is probably acrylate paint. A thin layer of repair mortar had been applied over the paint. This mortar is not carbonated and contains lime filler.

There is an opaque layer on part of the concrete surface. The concrete near this opaque layer has a high frequency of micro-cracks (figures M-6 and M-7). This crack pattern indicates a rapid and local dynamic load. This damage is local and superficial. The occurrence of portlandite a few millimetres from this structure shows that the temperature has not been above 450°C. It is not the type of crack pattern that is formed by a high-temperature event such as fire. The opaque layer is probably a repair

material. The damage is probably due to mechanical impact. It had been repaired with the same type of mortar as covers the rest of the concrete surface on the two samples.

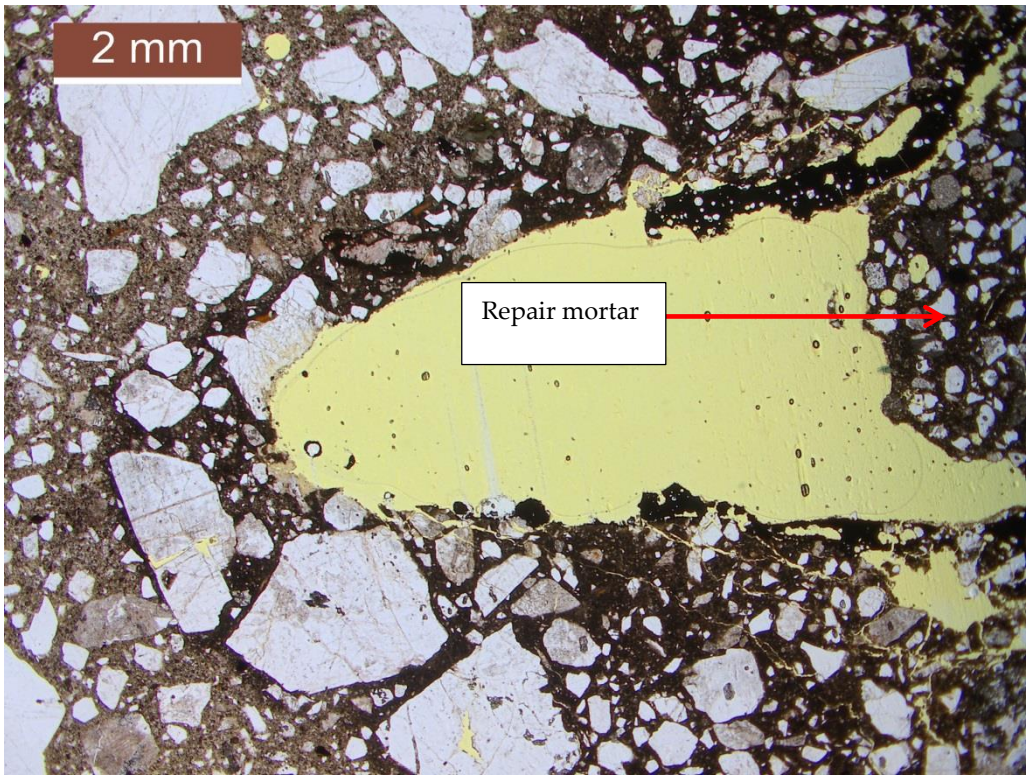

Figure M-6. Shows the damaged area. Thin section image taken in plain light.

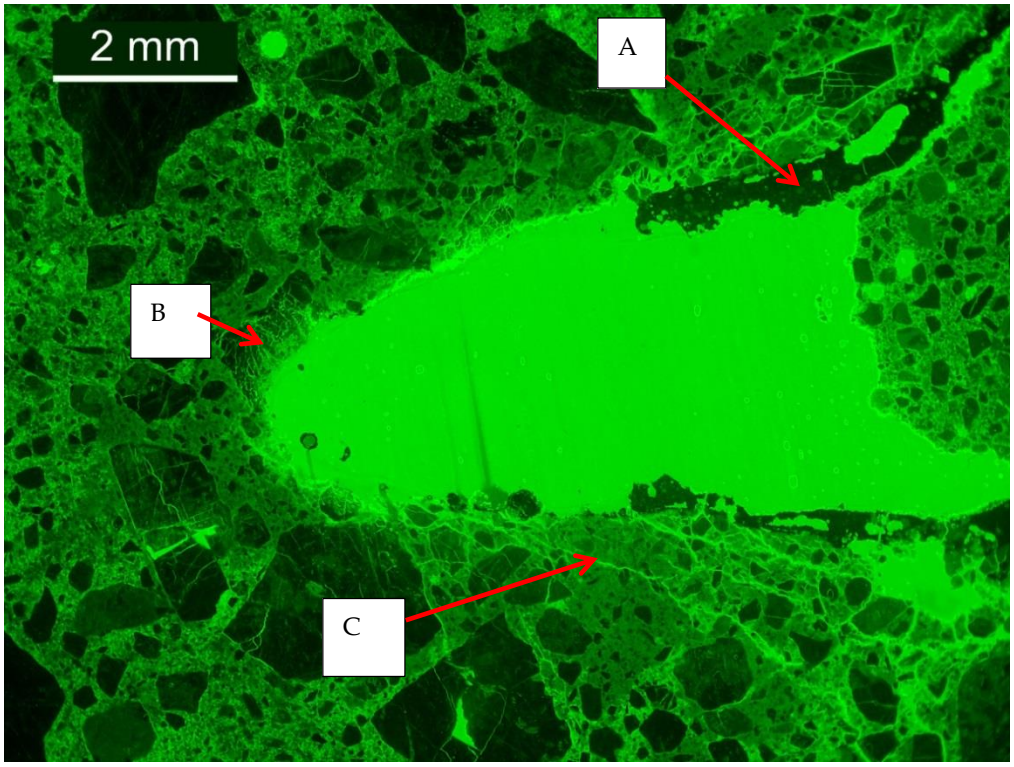

Figure M-7. The same area as in the figure above. The image is taken in fluorescent light. A is probably a repair material. B marks aggregate with a very large number of micro-cracks. C is an area with fine cracks in the cement paste. In this image porous materials are shown in brighter green and denser materials in darker green. Cracks and pores are shown in bright green.

5.2.1 Scanning electron microscopy

The micro-chemical analysis showed a normal chemical composition for the cement paste (table M-1). The chloride content is near or below the detection limit for the method. The chloride content from this method cannot be directly compared with those obtained from titration. The determination of the oxygen content has a very high uncertainty. Aluminium through calcium and silica through calcium ratio (Al/Ca respectively Si/Ca) given in table M-1 shows a normal range. Normally the Si/Ca ratio is approximately 0.35 and the Al/Ca ratio is slightly below 0.1. The sulphur content is normally approximately 0.7%.

Micro-chemical analyses from the damaged area in sample core 5 are shown in table M-2.

Table M-1. Micro-chemical analyses in the outermost 1.5 mm of the concrete and analyses obtained about 20 mm in from the concrete surface.

	Na	Mg	Al	Si	S	Cl	K	Ca	Fe	O	Al/Ca	Si/Ca
Average surface	0.3	0.8	3	12	0.9	0.2	0.6	44	2	36	0.08	0.29
Standard deviation	0.3	0.4	2.3	4.8	0.5	0.1	0.4	7.8	2.2	2.6	0.07	0.18
Average inner	1.1	1.3	3	14	0.6	0.2	0.9	38	2	38	0.08	0.38
Standard deviation	0.5	1.4	1.7	3.0	0.3	0.1	0.3	5.2	3.4	1.7	0.06	0.09

Table M-2. Analyses in the opaque material in the damaged structure. The results are given as weight percentage.

Na	Mg	Al	Si	S	Cl	K	Ca	Fe
1.1	0	2	13	0	0	2	18	31
2	0.6	3	10	0	0	0.8	8	44
1.4	0.4	3	15	0	0	1.3	15	27
1.5	0.6	4	11	0	0	1.0	12	39
6.7	0	1	9	12	0	19	12	1.0
0.7	0	13	22	0	0	0.4	17	1.2
5	0	2	8	9	0	9	26	2
2	0.4	3	15	0.7	0	2	27	13
3	0.5	3	14	0.7	0	1.3	29	12

6 Compression tests

6.1 TEST SET-UP AND PERFORMANCE

The mechanical properties of the concrete were evaluated by uniaxial compression tests on cylinders machined from drilled cores. The cylinders were taken out from the parts of the cores closest to the surface of the structure, which was free from reinforcement. The cylinders were cut and flat-ground to final length, see Figure T-1.

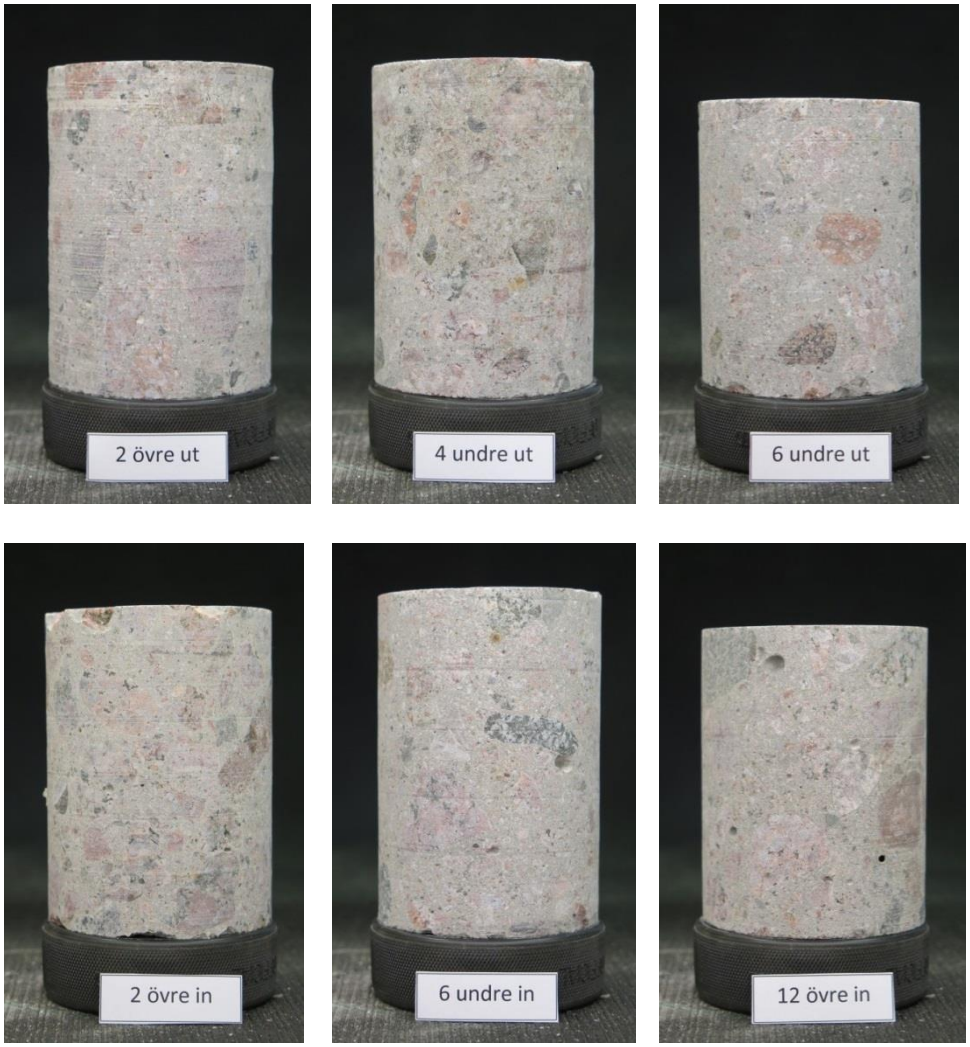

Figure T-1. Photos of the prepared test cylinders before testing. The three upper samples labelled “ut" are taken close to the outside of the structure, and the three lower samples labelled “in" are taken close to the inside of the structure.

The tests were carried over the period 10/11/2014–12/11/2014, in the mechanical laboratory at SP Structural and Solid Mechanics. The uniaxial compression tests were carried out in a servo-hydraulic testing machine under deformation control at a rate of 0.1 mm/min. Photo of the test set-up is shown in Figure T-2.

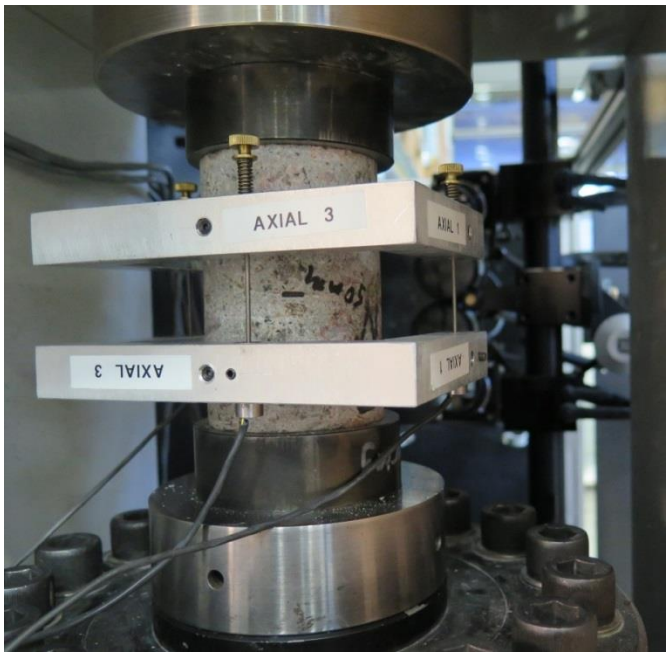

Figure T-2. Experimental test set-up with optical measuring system in the background.

The axial load, *F*, was measured with a load cell with a rated capacity of 1.5 MN and accuracy within 1%. The cylinders were oriented so that the loading area that was located closest to the surface of the structure (inside or outside) was placed against the lower loading plate. The axial stress is defined as:

$$\sigma = \frac{F}{A} \tag{1}$$

where A is the cross-sectional area of the cylinder. The deformation δ was determined as the average of three inductive sensors with a gauge length l_g of 50 mm. The sensors had a measurement range of ±2.50 mm and a relative error less than 1%. The axial strain is defined as:

$$\varepsilon = \frac{\delta}{l_g} \tag{2}$$

Full-field strain measurement was performed on the surface of the cylinders during the compression test. The optical full-field deformation measurement system ARAMIS™ 12M by GOM was used. The system uses a measurement technique based on Digital Image Correlation (DIC) with a stereoscopic camera set-up, consisting of two CCD cameras with 12 megapixel resolutions. The basic idea behind DIC is to measure the deformation of the specimen during testing by tracking the deformation of a surface speckle pattern in a series of digital images acquired during loading. This is done by analysing the displacement of the pattern within discrete facet elements of the image.

The system was calibrated for a measurement volume of approximately 155 × 120 × 70 mm³. A facet size of 50 × 50 pixels and a 10 pixel overlap along the circumference of each facet were chosen. This corresponds to a spatial resolution of approximately 2 × 2 mm² and an accuracy in coordinate measurements better than 1 µm.

6.2 RESULTS

A comparison of the measured stress-strain relationships is shown in Figure T-3. The compressive strength f_c was evaluated as the maximum axial stress and the modulus of elasticity E_c was evaluated from the stress-strain relationship as the secant modulus between 5 MPa and $f_c/3$. Table T-1 presents a summary of the determined concrete material properties.

Although there is a relatively large variation in compressive strength between the samples, the average compressive strength and average modulus of elasticity show no significant difference between cylinders taken close to the inside and close to the outside of the structure.

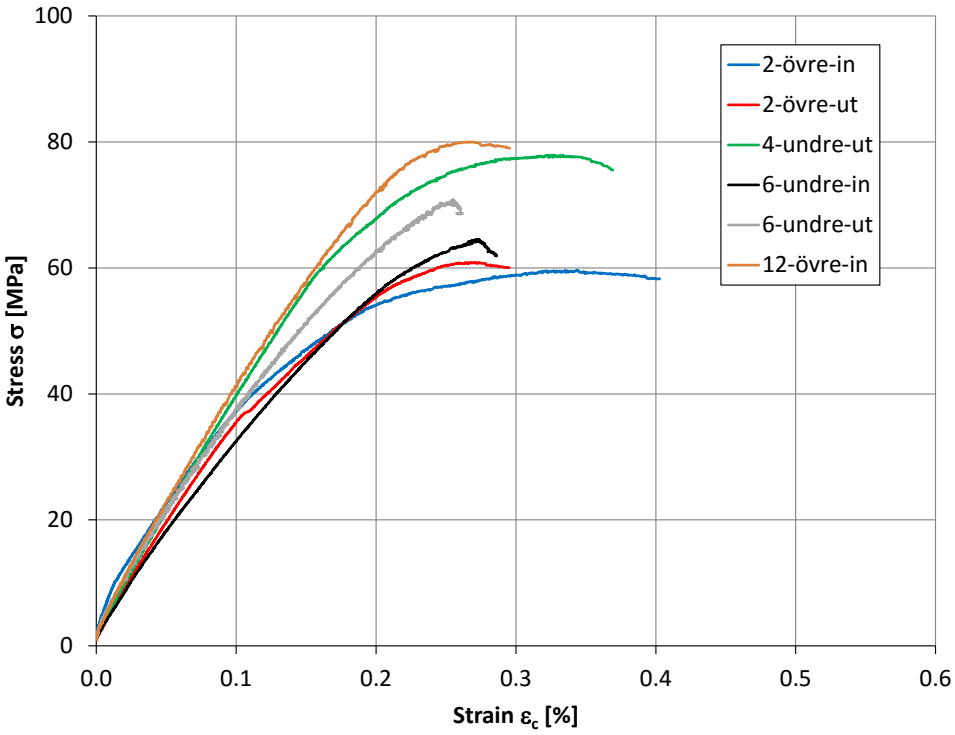

Figure T-3. Stress-strain relationships for the tested cylinders.

Table T-1. Summary of test results.

Sample id.	Diameter [mm]	Height [mm]	E_c [GPa]	f_c [MPa]
2-övre-ut	73.5	102.7	36.3	60.9
4-undre-ut	72.5	103.7	39.0	77.9
6-undre-ut	72.6	91.7	36.7	71.5
		Average	***37.3***	***70.1***
		Std. dev.	***1.4***	***8.6***
2-övre-in	73.6	101.1	38.4	59.6
6-undre-in	72.7	106.7	32.5	64.5
12-övre-in	73.4	95.5	39.6	80.1
		Average	***36.8***	***68.1***
		Std. dev.	***3.8***	***10.7***

The deformation field evaluated from the optical measurement system was used to quantify how the possible mechanical degradation of the concrete changes with the distance from the surface of the structure, by analysing the stiffness change in segments along the drilled cores. The measurement area was divided into nine 10 mm high segments defined by ten evenly spaced sections, see Figure T-4. The first section was placed approximately 5 mm from the lower loading area. The axial displacement of each facet element along the sections was exported from the optical measurement system, see Figure T-5. The strain in each segment $\varepsilon_{c,s}^{m-n}$ was then calculated as the difference between the mean values of the axial displacement δ_m^n and δ_m^m of the corresponding sections n and m, respectively, divided by the initial distance l_0 between the sections as:

$$\varepsilon_{c,s}^{m-n} = \frac{\delta_m^n - \delta_m^m}{l_0} \quad (3)$$

Figures T-6 and T-7 show the distribution of axial compressive strain in the various segments of the cylinders taken towards the outside and towards the inside of the structure, respectively. For all samples, the strain distribution was evaluated at a compressive stress of 23 MPa, which approximately corresponds to $f_c/3$, the level at which the modulus of elasticity was evaluated as described above.

That there is some variation in strain between the various segments is natural, since the local stiffness depends on aggregate size and location. The general picture is that the strain distribution is relatively uniform along the length of the cylinder, which indicates that the tested cylinders do not exhibit any degradation of mechanical properties. There is also no significant difference between the cylinders taken towards the inside of the structure, compared with those taken towards the outside, even if the cylinders towards the inside, on average exhibit somewhat lower strains, i.e. higher stiffness, see Figure T-8.

The overall conclusion is that the tests carried out do not indicate any degradation of the mechanical properties, and that the properties in general are equivalent for the cores taken towards the inside and the outside of the structure.

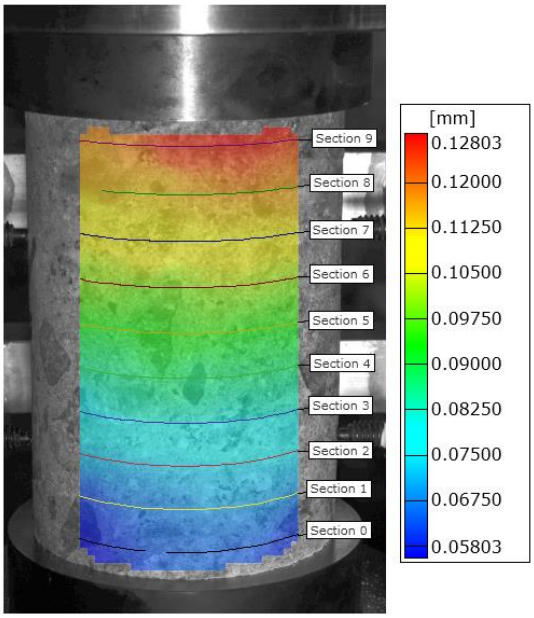

Figure T-4. Example of deformation field for cylinder "4-undre-ut" at an axial compression stress of 23 MPa.

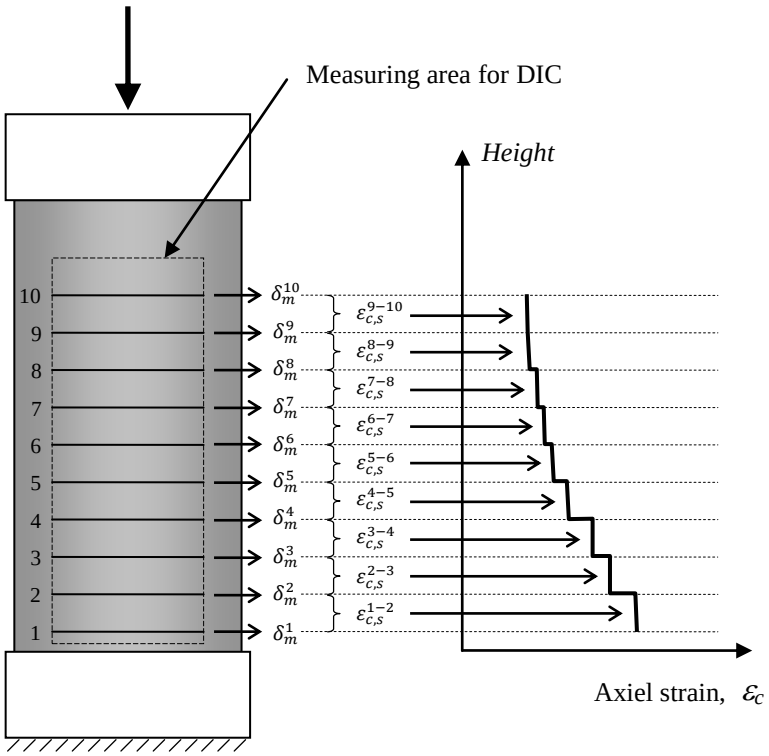

Figure T-5. Illustration of the evaluation of the compressive strain by dividing the cylinder into segments.

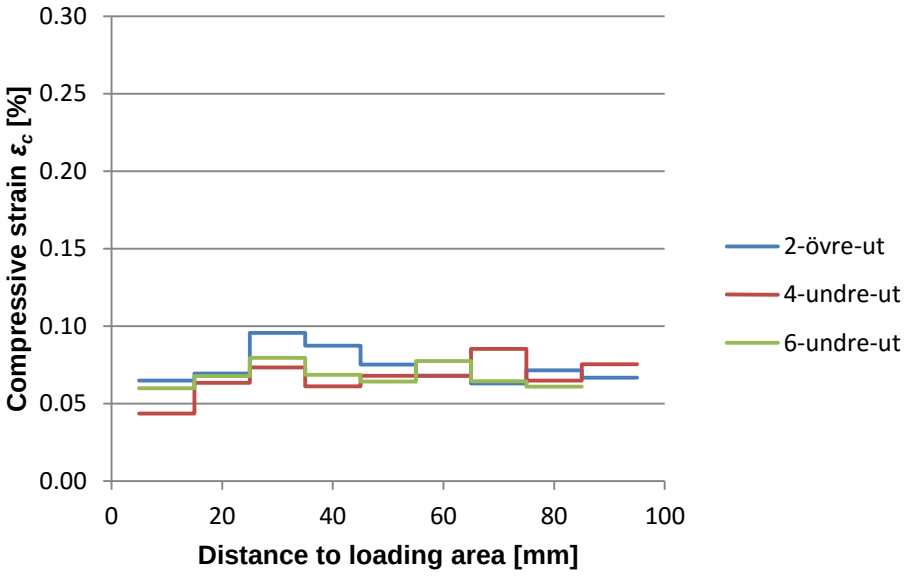

Figure T-6. Axial compressive strain in the different segments $\varepsilon_{c,s}$ as a function of the distance from the lower loading area, for the cylinders taken towards the outside of the structure.

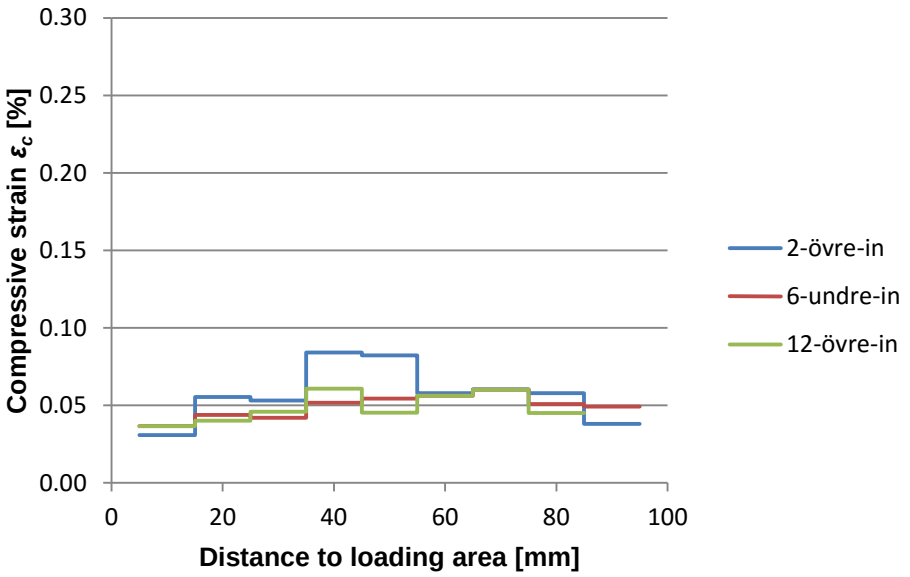

Figure T-7. Axial compressive strain in the different segments $\varepsilon_{c,s}$ as a function of the distance from the lower loading area, for the cylinders taken towards the inside of the structure.

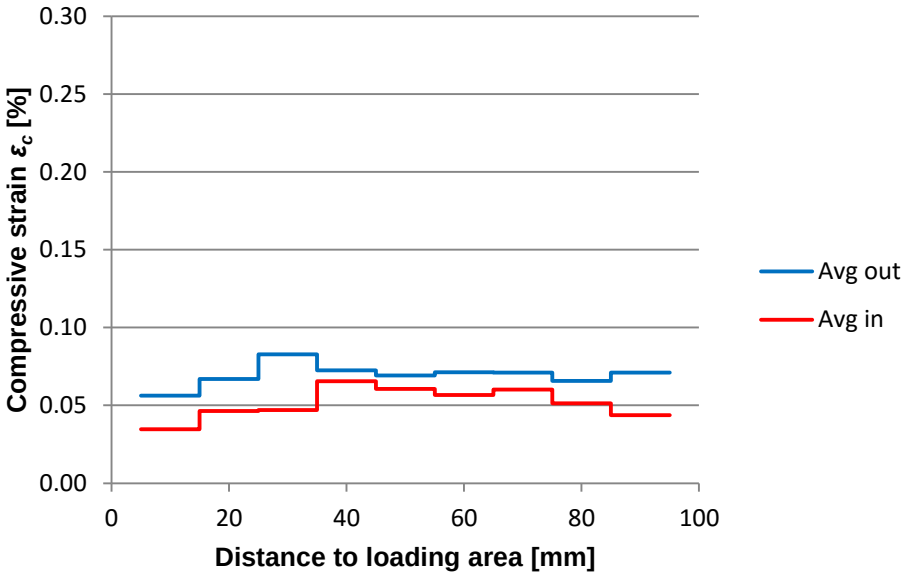

Figure T-8. Axial compressive strain in the different segments $\varepsilon_{c,s}$ as a function of the distance from the lower loading area, represented as average curves for cylinders taken towards the inside (red) and outside (blue) of the structure.

7 References

Flansbjer M, Lindqvist JE & Silfwerbrand J 2011: Quantitative fracture characteristics in shear load. Fib Symposium Prague 2011, 12pp.

Hilsdorf HK, Kropp J, & Koch HJ 1978 "The Effects of Nuclear Radiation on the Mechanical Properties of Concrete" ACI SP 55-10 223-251, 1978.

Ichikawa T & Koizumi H 2002 "Possibility of Radiation-Induced Degradation of Concrete by Alkali-Silica Reaction of Aggregates". Journal of Nuclear Science and Technology, Vol. 39, No. 8, p. 880–884.

Kaspar W, Yunping Xi, Naus D & Graves HL 2013 "A review of the Effects of Radiation on Microstructure and Properties of Concretes Used in Nuclear Power Plants" USNRC 2013, http://www.nrc.gov/reading-rm/doc-collections/nuregs/

Le Pape Y, Field KG & Remec I 2015 "Radiation effects in concrete for nuclear power plants, Part II: Perspective from micromechanical modelling" Nuclear Engineering and Design Vol. 282, 144–157.

Ljustell P and Wåle J 2014 "Degradering av betong och armering med avseende på bestrålning och korrosion" SSM rapport 2014:31, http://www.stralsakerhetsmyndigheten.se/Global/Publikationer/Rapport/Sakerhet-vid-karnkraftverken/2014/SSM-Rapport-2014-31.pdf

Maruyama I, Kontani O, Sawada S, Sato O, Igarashi G & Takizawa M 2013 "Evaluation of Irradiation Effects on Concrete Structure: Background and Preparation of Neutron Irradiation Test." ASME 2013.

NT BUILD 361 Concrete Hardened Water Cement Ratio. Nordtest Method Approved 1999-11.

Saouma VE & Hariri-Ardebili MA 2014 "A proposed aging management program for alkali silica reactions in a nuclear power plant" Nuclear Engineering and Design vol. 277, 248–264.

ANALYSIS OF IRRADIATED CONCRETE

Irradiation effects on concrete is a subject that has drawn more and more attention, as the possible life time extension of nuclear power plants beyond original design life is discussed.

The overall conclusion of the analysis made on drilled concrete cores is that the tests carried out do not indicate any degradation of the mechanical properties. The recorded changes in concrete properties are comparable with what would be expected in a non-concrete aggressive indoor environment. No degradation due to radiation, such as volume changes or alkali silica reactions, could be identified.

Another step forward in Swedish energy research

Energiforsk – Swedish Energy Research Centre is a research and knowledge based organization that brings together large parts of Swedish research and development on energy. The goal is to increase the efficiency and implementation of scientific results to meet future challenges in the energy sector. We work in a number of research areas such as hydropower, energy gases and liquid automotive fuels, fuel based combined heat and power generation, and energy management in the forest industry. Our mission also includes the generation of knowledge about resource-efficient sourcing of energy in an overall perspective, via its transformation and transmission to its end-use. Read more: www.energiforsk.se

Energiforsk